UCRL-JC-139459
PREPRINT

NIF-scale hohlraum asymmetry studies using point-projection radiograph of thin shells

Steve Pollaine, David Bradley, Otto Landen, Russell Wallace, Ogden Jones, Peter Amendt, Larry Suter and Robert Turner

Lawrence Livermore National Laboratory
Livermore, CA 94550

This paper was prepared for submittal to
42nd Annual Meeting of the APS Division of Plamsa Physics
Quebec City, Canada
October 23-27, 2000

October 18, 2000

NIF-scale hohlraum asymmetry studies using point-projection radiograph of thin shells

Steve Pollaine, David Bradley, Otto Landen, Russell Wallace,
Ogden Jones, Peter Amendt, Larry Suter and Robert Turner
Lawrence Livermore National Laboratory

Introduction

The National Ignition Facility (NIF) is a 192 beam, 2 MJ 0.35 μm laser now being built at Lawrence Livermore National Laboratory [1]. NIF is designed to drive inertial confinement fusion (ICF) capsules to ignition using indirect drive, in which the laser energy is converted to thermal x rays inside a cavity (hohlraum). The x rays then ablate the outer layers of a capsule inside the hohlraum, causing the capsule to implode and achieve ignition. One of the major sources of possible failure to achieve ignition is x-ray flux asymmetry on the capsule. All flux asymmetry can be analyzed in terms of the spherical harmonics Y_{lm}. If the flux is azimuthally symmetric (only m=0 components), the flux asymmetry can be expressed in terms of Legendre polynomials P_l In this paper, we will describe flux asymmetry in terms of the Legendre polynomial coefficients a_l.

Because the hohlraum is symmetric about the midplane, odd Legendre modes are zero in the absence of pointing errors and power imbalance. Because higher modes are smoothed out by radiation transport from the hohlraum walls to the capsule (with a transfer function that goes roughly as mode$^{-2.5}$[2]), we are most concerned with diagnosing and controlling P2, P4, P6 and P8 flux asymmetry.

Fig. 1 shows a typical NIF ignition capsule and the temperature drive. Typically, three or four shocks keep the DT fuel on a low adiabat, so that the capsule reaches roughly 1000 g/cc at ignition time. 2-D integrated radiation-hydrodynamics simulations show that the capsule will fail when the average Legendre coefficient a6 is greater than 1%, or when a8 is greater than 0.6%. To provide for some margin of error, we have set the NIF specifications on flux asymmetry as a2/a0 < 1.0%, a4/a0 < 0.5%, a6/a0 < 0.3 %, and a8/a0 < 0.25%. [3]

Asymmetry Diagnostics

A variety of different techniques measure the symmetry in hohlraums using surrogate capsules. The reemission ball [4] is a solid Bi ball with the same radius as an ICF capsule. Thermal radiation on the ball heats it up, and it reemits the radiation at its characteristic temperature, which will vary from point to point on the ball if the incoming flux is asymmetric. When viewed in 2 KeV x rays, the emission from the ball is highly sensitive to the temperature, and thus is sensitive to the incoming flux. Thus small variations in temperature are magnified, and can be measured as a function of time.

Another asymmetry diagnostic is the foam ball [5]. This is a solid sphere of low-density SiO_2 or CH. A converging shock produces a visible limb, and the radius of the limb as a function of angle gives information about the incoming flux asymmetry as a function of time. The speed of the shock varies as the square root of the incident flux.

A third asymmetry diagnostic is the imaging of imploded cores from a symmetry capsule. For example, spherical hohlraums with tetrahedral illumination (four laser entrance holes) have yielded triangular implosion images [6], showing that the part of the capsule that lies under a laser entrance hole feels a reduced flux.

In this paper, we will concentrate on the thin shell diagnostic. Table 1 below compares the demonstrated accuracy of the various techniques for P2, P4, P6 and P8.

Table 1. Experimental accuracy demonstrated at Nova/Omega, scaled to NIF, for the four asymmetry diagnostics discussed in this paper. The first column is the accuracy to a P2 perturbation that lasts for 2 ns. The remaining columns show both the accuracy to a perturbation on the foot only, and the response to the perturbation being constant for all time.

	P2,2 ns Foot (all)	P2 Foot (all)	P4 Foot (all)	P6 Foot (all)	P8 Foot (all)
NIF ignition requirement	10% (10%)	2% (1%)	1% (0.5%)	0.7% (0.33%)	0.5% (0.25%)
Reemission ball	3%				
Foam Ball	5% (2.5%)	0.5% (0.5%)	0.6% (0.6%)		
Imploded Core		0.25% (0.25%)			
Thin Shell		0.5%	0.6%	0.7%	0.8%

Thin shell asymmetry diagnostic

The thin shell diagnostic is a capsule 2 to 3 mm in diameter, with a thickness of 10 to 15 μm of $CH_{1.3}Ge_{.076}$. Because the acceleration is proportional to the ablation pressure divided by the areal mass density $\int \rho dr$, and $\int \rho dr$ is approximately conserved during the implosion, the shape of the thin-shell capsule reflects the drive asymmetry. Thus there is less non-linear coupling between the different modes, compared to shock-driven surrogates such as solid foam balls. This is important because big swings in P2 won't couple to the modes we want to measure.

A useful measure of linearity is the coefficient c in $\frac{dr}{r} = c\frac{d\,\mathrm{Pr}}{\mathrm{Pr}}$, where r is the measured radius or any other measured variable and Pr is the pressure driving the implosion. In a strictly linear system, c = 1. For a foam ball, c = 1/2. For the reemission balls, we replace radius and pressure with the fluorescent flux at 2 KeV and incoming flux on the capsule. For a pure blackbody, F~exp(-hv/kT), so that $\frac{dF}{F} = \frac{1}{4}\frac{hv}{kT}\frac{dT^4}{T^4}$. For a 200 eV hohlraum, then c = 2.5. For a thin shell, c = 1 as long as $\int \rho dr$ is constant. This approximation is good, as effects of convergence tend to cancel the effects of mass ablation, until the radius of the shell has converged at least half way.

Another way that nonlinearity could develop is if mass flowed in a transverse direction. Because the shell thickness is much less than the wavelengths of interest, there is no Rayleigh-Taylor amplification of those wavelengths and thus virtually no transverse mass flow.

In a thin shell, the outer part of the shell ablates, compressing the inner part of the shell. This produces a 1.2 to 1.4 Mb shock with a velocity jump of 8 to 9 km/s. When the shock reaches the inside edge of the shell, the shell starts accelerating. The motion of the dense shell is then given by

$$\Delta r = r_0 - r(t) = v_0(t - t_0) + \int_{t_0}^{t} g(t')(t - t')dt', \quad g \propto \frac{\mathrm{Tr}^{3.5}}{\int \rho dr}$$

where $r_0 \sim 0.8$ mm, $v_0 \sim 9$ km/s and $t_0 \sim 1.4$ ns. Note that the radial position of the shell is most sensitive to early asymmetry, around the time when the shock breaks out of the shell. As the shell implodes, distortions caused by flux asymmetry will continue to grow.

The thickness of the shell can be varied to change the sampling time. However, if the shell is too thin, the Rayleigh-Taylor instability (with modes > 400) will break up the shell, and resolution of the limb will suffer. Our experiments suggest that a thickness of 15 μm is optimum for the experiments we are doing on the Omega laser at the Laboratory for Laser Energetics at the University of Rochester.

We can increase the capsule/case ratio to enhance the effect of high-order flux asymmetries. Fig. 2 shows the radiation transfer function for a capsule within a spherical case for a capsule/case radii ratio of 0, 0.2, 0.4, and 0.6 in modes 0 through 8. Note that by increasing the capsule/case ratio from a NIF-like value of 0.4 to 0.6, the sensitivity to modes 6 and 8 are increased by an order of magnitude. The transfer function for a sphere inside a cylinder, the usual hohlraum shape, is more complicated because the Legendre polynomials and spherical harmonics are no longer the normal modes. However, when cross-coupling between modes is taken into account, there is still an order of magnitude increase in flux sensitivity to the higher modes with the higher capsule/case ratio.

2-D radiation-hydrodynamics simulations [7] show that a thin shell is sensitive to thickness variations, but not to ripples on the surface that keep the thickness constant. A 0.1 μm variation in thickness in a 15 μm shell that travels 200 μm will cause an amplitude of 1.3 μm in radius, just below the limit of detectability.

Experiments on Omega

We have run four sets of experiments with the thin shell diagnostic at the 60-beam Omega laser at the Laboratory for Laser Energetics at the University of Rochester. Fig. 3 shows the basic arrangement. The hohlraum is driven by several rings of laser beams at 23, 48, 59 and 62 degrees relative to the hohlraum symmetry axis. 24 of the 60 beams heat the hohlraum from 0 to 3 ns, and another 18 beams continue the heating from 3 to 6 ns. Some of the remaining beams drive a Ti backlighter, which stands just behind two 50 μm pinholes. The light goes through two viewports on the side of the hohlraum, illuminates the thin-shell capsule, and projects onto a two frame gated camera. One pinhole is illuminated around 3 ns, and the other is illuminated around 7 ns, to produce two snapshots of the thin shell as it implodes. The overall time resolution is 240 ps, and the magnification of the image has varied from 5 to 8. The viewports on the hohlraum are covered with 0.5 μm of Au to keep up the albedo and reduce the effect of the holes on the capsule.

Over the past two years, we have improved our image quality. Backlit pinholes produce a much higher signal/noise ratio than area backlighters. By dividing our images by the flat field of the detector, we have gained a 20% improvement in the measurement of the position of the limb. Fig. 4 shows two pictures of one capsule taken 4 ns apart.

The limb position is analyzed as a function of angle. The observed width of the limb, shown in fig. 5, is consistent with our simulation with 50 μm pinholes. Fig. 6 compares late-time (6.7 ns) data from a 15 μm shell with a

2-D integrated radiation-hydrodynamic simulation [7]. There is good qualitative correspondence of various features between experiment and simulation.

Error analysis

There are three main sources of error in the measurements. There is a random measurement error of about 2 μm per measurement. When averaged over 100 independent measurements, the random error is then $0.2\sqrt{2l+1}$ μm per mode. When divided by the distance traveled, typically 200 μm, the error bar for a given Legendre coefficient a_l/a_0 is then $\sqrt{2l+1}$ 0.1%. This is adequate for meeting the NIF specifications for the foot only. Over the main part of the pulse, with a 300 eV drive temperature, a thin shell capsule can be imploded by 700 μm, with an error bar of $\sqrt{2l+1}$ 0.03 %. This is a factor of two better than what is required for meeting the NIF specification of 0.25% for P8, the most stringent case.

Another source of error comes from fabrication defects. If the thin shell has a 1% variation in thickness or density, then the distance moved will also vary by 1%. Current capsules have a thickness variation of 0.2 to 0.8 μm out of a total thickness of 15 μm, almost entirely in a P1 defect – like an off-centered sphere. A pure P1 defect will not affect the measurements because to first order it is equivalent to a displacement of the center of the image, and we remove this defect before we analyze our data. We currently do not know the spectrum of thickness variations, but we plan to measure these variations with interferometry and throw away the bad thin-shell capsules.

A third source of error comes from laser pointing errors and laser power imbalance. Fig. 7 shows the results of calculations made with the 3-D viewfactor code GERTIE. For two of the Omega shots in February 2000, a 10 μm shell (shot 19082) and a 15 μm shell (shot 19083), the actual beam energies of each of the 42 beams entering the hohlraum were taken and used to modulate the power going to the hohlraum wall proportionately. The viewfactor code then calculated the resulting flux on the capsule. The line of sight from the pinhole to the detector defines a great circle around the capsule which corresponds to the limb as seen in the images. The flux along this limb was then compared in two cases: (1) the full 3-D version and (2) a 2-D version in which each beam became an azimuthally symmetric ring. Fig. 7 compares the 2-D with the 3-D version of the code. Note that the 2-D and 3-D versions are similar for shot 19083, but not for shot 19082. In shot 19082, one of the beams had only 130 J, compared to the average of all the other beams of 248 J. This particular beam, unfortunately, was on the limb relative to the line of sight, at an angle of 44 degrees as seen from the capsule. This accounts for the large negative feature at around 300 degrees seen in the 3-D calculation. Thus the thin-shell technique requires decent power balance.

The two shots differed in one other significant way as well. Shot 19083, with the 15 μm thick shell, showed a random measurement error of 5 μm at 6.7 ns, whereas shot 19082, with the 10 μm thick shell, showed a random measurement error of 13 μm at 6.7 ns. We believe this suggests that the thinner shell started breaking up due to the Rayleigh-Taylor instability, whereas the thicker shell remained intact.

Extension to NIF

How will these sensitivities extend to NIF? The sensitivity of each Legendre coefficient is given by $\frac{\Delta a_l}{a_0} \approx \frac{\sqrt{2l+1}\sigma_{\rm rms}}{\Delta r\sqrt{n}}$, with n the number of independent measurements of the limb position and Δr the distance traveled by the shell at the time of measurement. To calculate a rough value for Δr, we employ a simple model in which the acceleration g is constant. Then $\Delta r = 0.5\ gt^2$, with g proportional to ablation pressure / ρd, with d the thickness of the shell. The ablation pressure is proportional to the radiation drive temperature to the 3.5 power. We note that the shell thickness d must be thick enough to avoid Rayleigh-Taylor breakup of the shell; thus Δr /d must be some fixed value c. Substituting $d= c\Delta r$ yields the relation $\Delta r \sim T^{1.75}\ t$. Table 2 below makes use of this relationship to give the expected sensitivity of the thin shell technique on NIF. Of course, it's important to make sure that the systematic errors from power imbalance and capsule fabrication are negligible.

Table 2. An extension of the Omega parameters to NIF shows that if we eliminate our systematic errors, and can maintain 2 μm accuracy in each measurement of limb position, then we can accurately measure asymmetry to better than NIF specifications.

	Omega	**NIF foot/spec**	**NIF peak/spec**
T (eV)	90	86	300
t (ns)	7	9	3
$(T/100)^{1.75}$ t	5.8	6.9	20.5
Δr(μm)	200	240	715
P2 sensitivity	0.22%	0.19% / 3 %	0.06% / 1%
P8 sensitivity	0.41%	0.34% / 0.75%	0.12% / 0.25%

Conclusions

Our current OMEGA experimental campaign is developing the thin shell diagnostic for use on NIF with the needed accuracy. The thin shell diagnostic has the advantage of linearity over alternative measurement techniques, so that low-order modes will not corrupt the measurement of high-order modes. Although our random measurement errors are adequate, we need to monitor beam balance and ensure that the thin shells have a uniform thickness.

Acknowledgements

We thank LLE, University of Rochester, for the use of the Omega laser. This work was performed under the auspices of the U.S. Department of Energy by the Lawrence Livermore National Laboratory under Contract No. W-7405-ENG-48.

References

[1] J.A. Paisner, J.D. Boyes, S.A. Kumpan, jW.H. Lowdermilk, M.S. Sorem, Laser Focus World **30**, 75 (1994).

[2] S.M. Pollaine, "Radiation Transport Between Two Concentric Spheres", accepted for publication, Nuclear Fusion (2000).

[3] Haan, private communication

[4] N.D. Delamater, G.R. Magelssen and A.A. Hauer, "Reemission technique for symmetry measurements in Hohlraum targets containing a centered high-Z ball", Phys. Rev. E **53**, 5240 (1996).

[5] P. Amendt, S.G. Glendinning, B.A. Hammel, O. Landen, and L.J. Suter, "Direct Measurement of X-Ray drive from Surrogate Targets in Nova Hohlraums", Phys. Rev. Lett. **77**, 3815 (1996).

[6] S.M. Pollaine, M.M. Marinak and D.H. Munro, "3-D Simulations of Tetrahedral Hohlraums", Bull. Am. Phys. Soc. **42**, 1993 (1997).

[7] G.B. Zimmerman and W.L. Kruer, Comments Plasma Phys. Control. Fusion **2**, 51 (1975).

Figure Captions

Fig. 1. NIF ignition capsule and its radiation drive temperature

Fig. 2. Radiation transfer function as a function of mode number for various capsule/case radii ratios. Note the huge enhancement in modes 6 and 8 in going to capsule/case = 0.6.

Fig. 3. Schematic of our experiment, and a picture of the hohlraum with its thin-shell capsule.

Fig. 4 Picture of the same thin shell 4 ns apart.

Fig. 5. A capsule limb profile

Fig. 6. Comparison of simulation with experiment on shot 19083

Fig. 7 Viewfactor calculations show that bad power imbalance can cause 3-D effects that disrupt the technique.

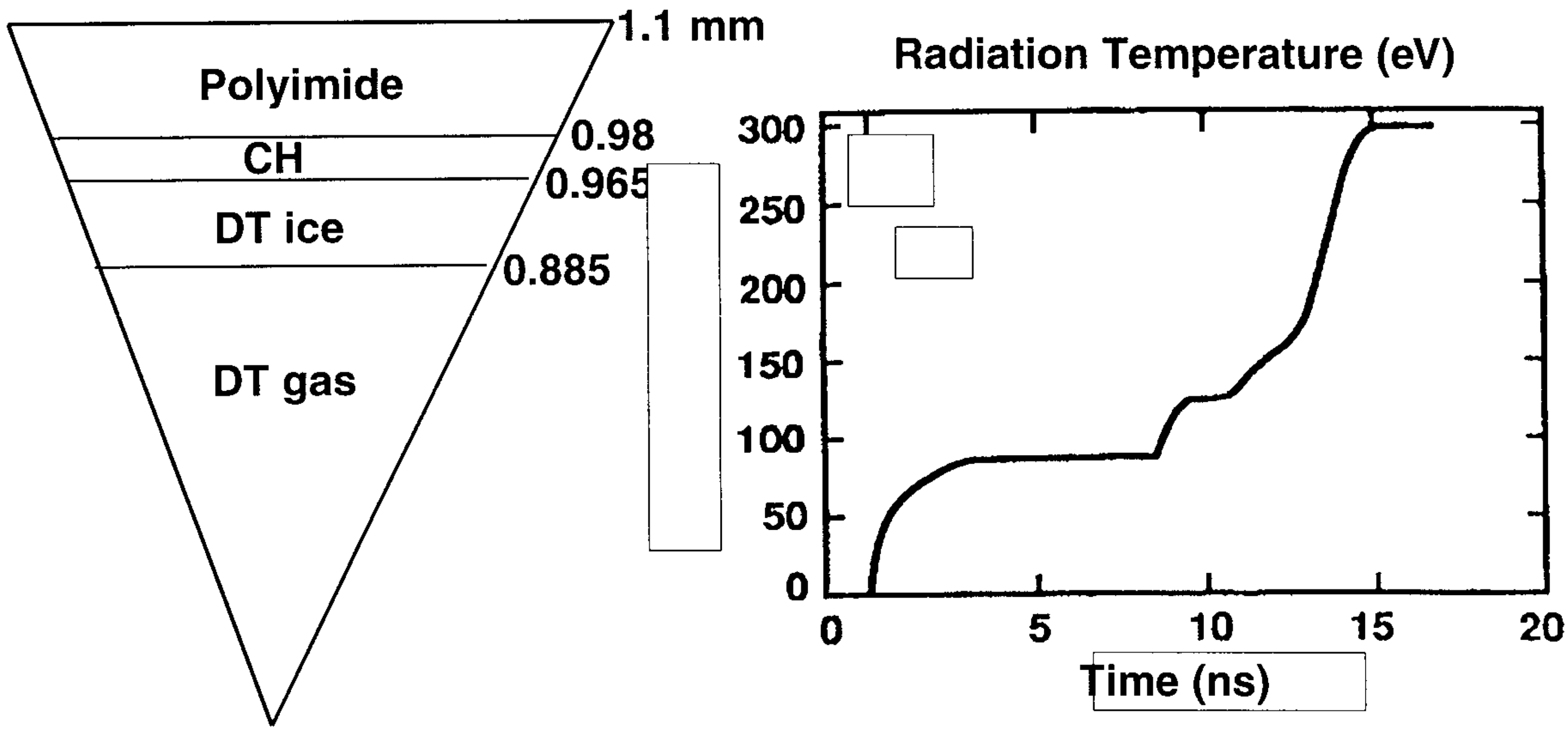

Fig. 1. NIF ignition capsule and its radiation drive temperature

Radiation transfer function

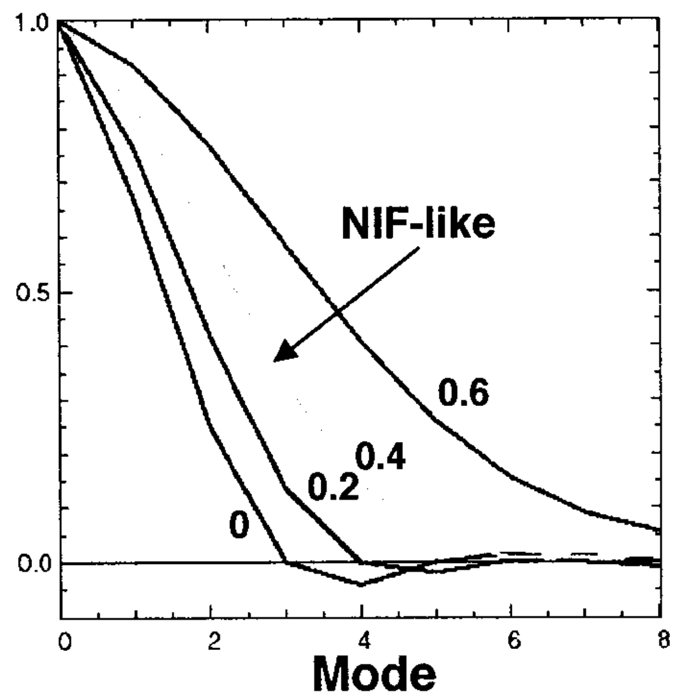

Fig. 2. Radiation transfer function as a function of mode number for various capsule/case radii ratios. Note the huge enhancement in modes 6 and 8 with capsule/case = 0.6.

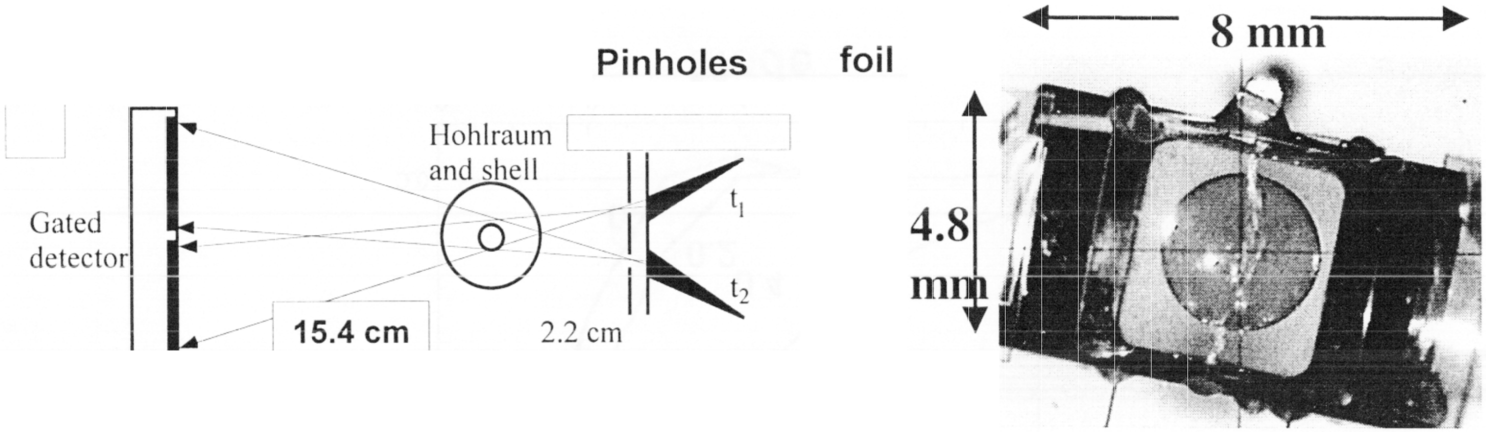

Fig. 3. Schematic of our experiment, and a picture of the hohlraum with its thin-shell capsule

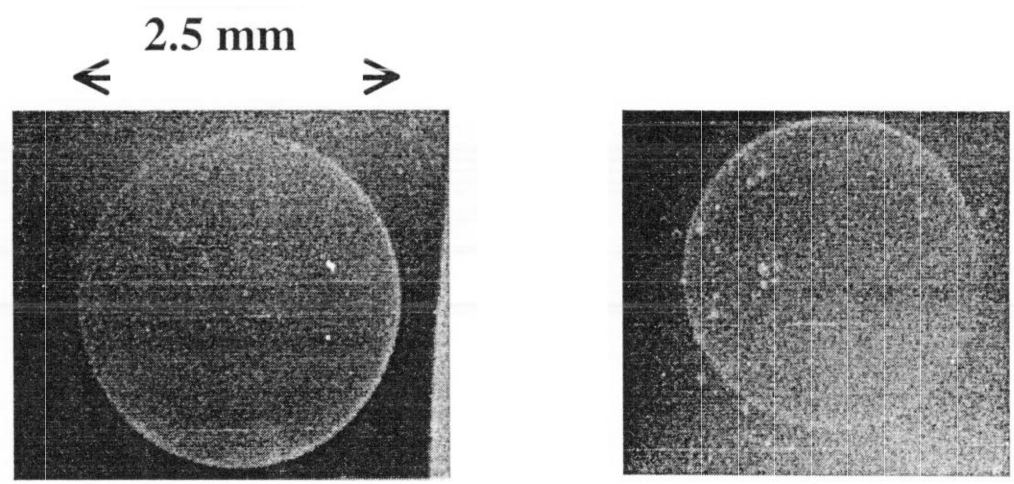

3.1 ns

$A_0 = 1245 \mu m$

7.1 ns

$A_0 = 1135 \mu m$

Fig. 4. Pictures of the same thin shell 4 ns apart.

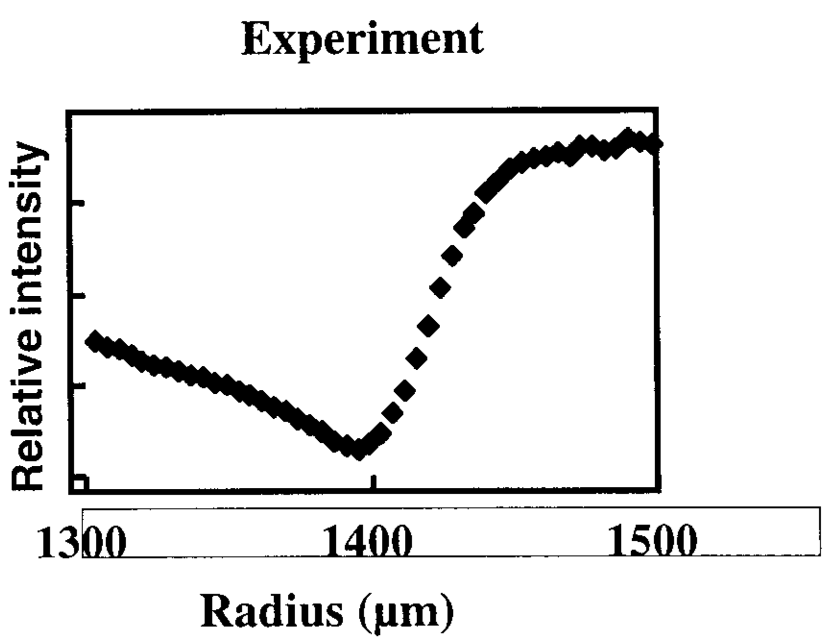

Fig. 5. A capsule limb profile

Shot 15632

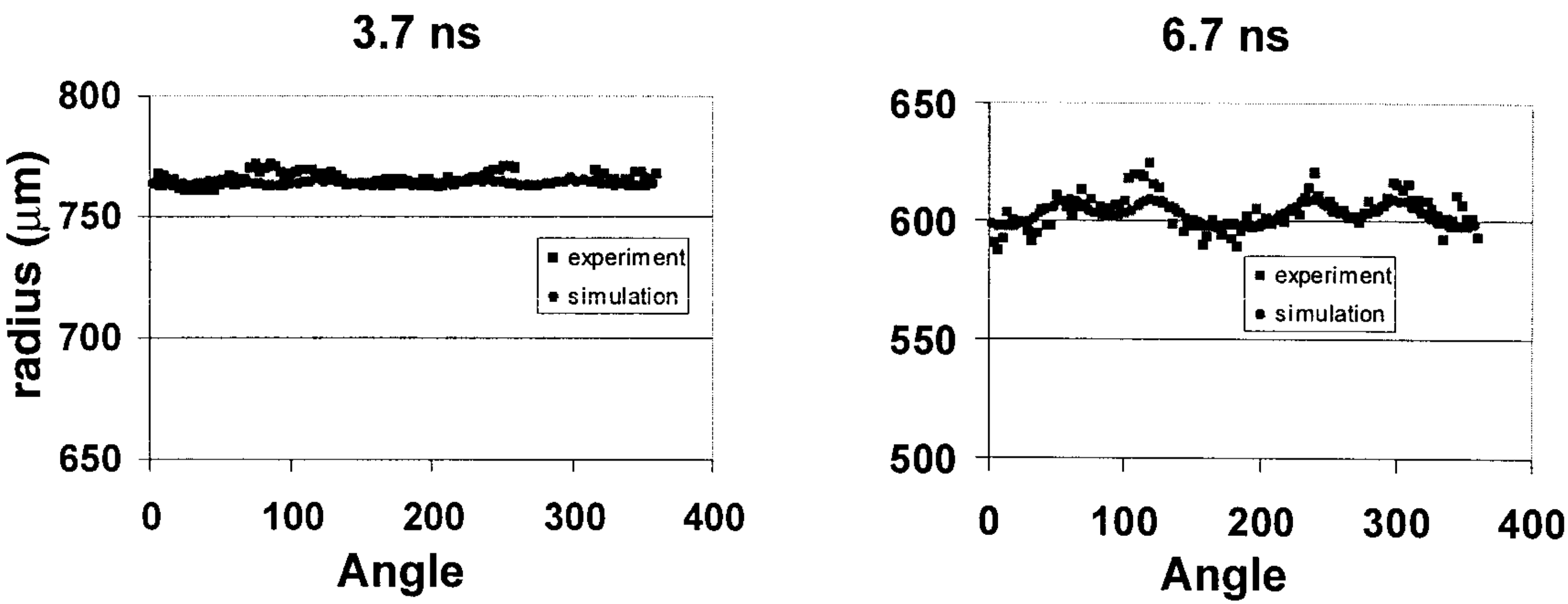

Fig. 6. A comparison of simulation with experiment on shot 19083 (15 μm thickness)

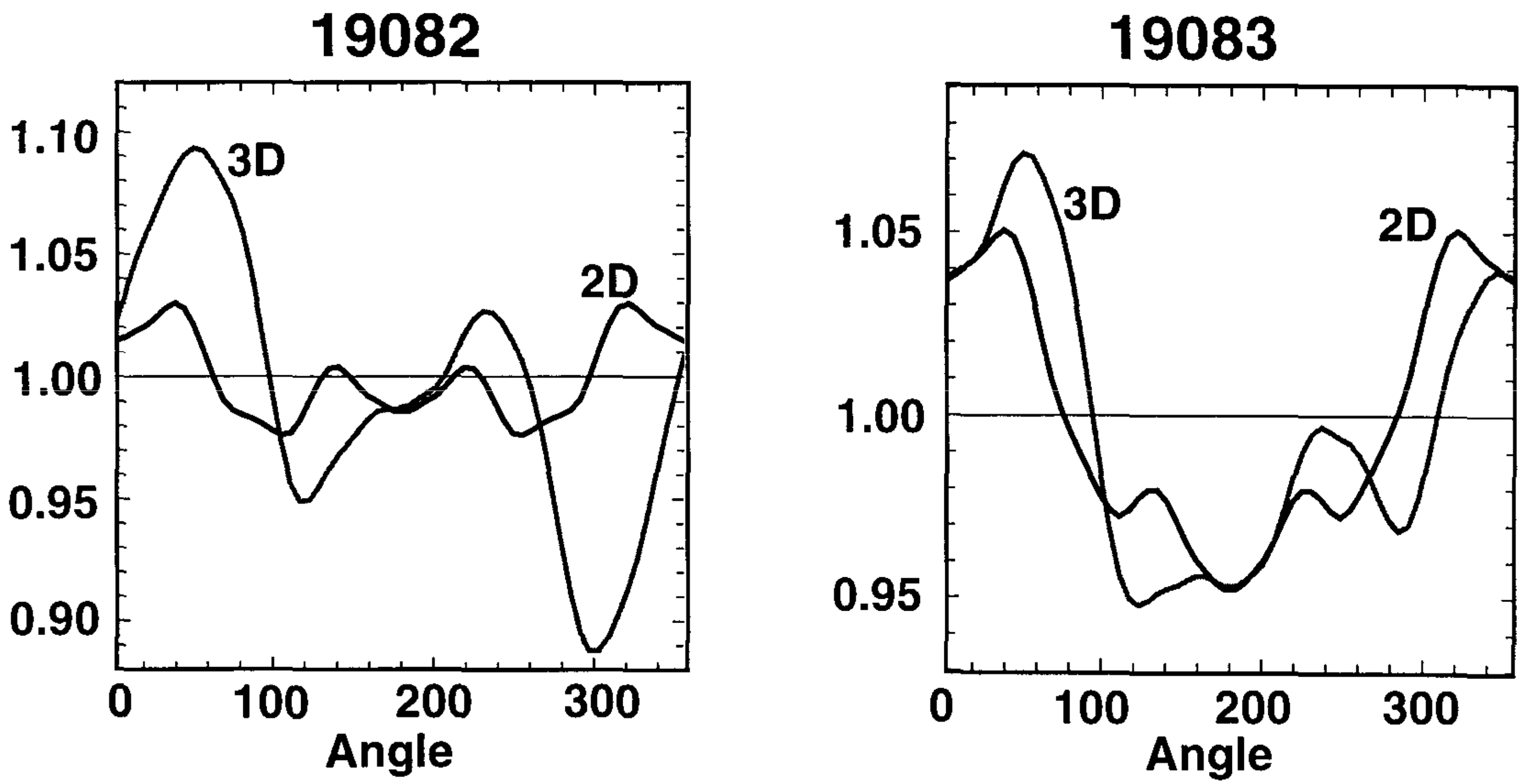

Fig. 7. Viewfactor calculations show that bad power imbalance can cause 3-D effects that disrupt the technique